Carbohydrate Polymers 86 (2011) 1602–1609

Contents lists available at ScienceDirect

Carbohydrate Polymers

journal homepage: www.elsevier.com/locate/carbpol

Fragrant chitosan nanospheres: Controlled release systems with physical and chemical barriers

Thapakorn Tree-udom[a,b], Supason P. Wanichwecharungruang[c,*], Jiraporn Seemork[a], Sunatda Arayachukeat[d]

[a] Program of Petrochemistry and Polymer Science, Faculty of Science, Chulalongkorn University, Bangkok 10330, Thailand
[b] National Center of Petroleum, Petrochemicals and Advanced Materials, Chulalongkorn University, Bangkok 10330, Thailand
[c] Department of Chemistry, Faculty of Science, Chulalongkorn University, Bangkok 10330, Thailand
[d] Program of Macromolecular Science, Faculty of Science, Chulalongkorn University, Bangkok 10330, Thailand

ARTICLE INFO

Article history:
Received 18 May 2011
Received in revised form 23 June 2011
Accepted 26 June 2011
Available online 6 July 2011

Keywords:
Chitosan
Fragrance
Controlled release
Nanospheres
Imine
Profragrance

ABSTRACT

Existing fragrance controlled release systems are either based on a physical barrier, such as entrapment of the fragrant molecules inside the micro- or nano-spheres, or a chemical barrier, such as labile chemical bonds. Here, we propose a system with a combination of the two approaches but fabricated *via* a simple surfactant free one step process using biodegradable chitosan polymer. The fabrication process involves a chemical reaction to covalently link the fragrant aldehydes with the amine functionalities of the N-succinylchitosan (NS-chitosan) carriers that simultaneously leads to an ultrasonic aided reorganization of the spheres in such a way that the grafted entities are at the particles' core. Localization of the grafted imine moieties at the core of the imine-NS-chitosan particles was confirmed by X-ray photoelectron spectroscopy (XPS) analysis. The obtained fragrant chitosan nanospheres not only showed up to 85-fold fragrance prolongation but also dispersed well in water.

1. Introduction

Current fragrance controlled release systems can be categorized into two groups, those that use (i) a physical barrier system in which the diffusion of the fragrant molecules are controlled by entrapping them into a polymeric matrix (carrier), and (ii) a chemical barrier system in which the fragrances are modulated *via* chemical derivatization into more robust forms but where this is reversible so that the fragrant molecules can be regenerated in a controllable manner (Herrmann, 2007). Both strategies have been employed in the flavor & fragrance industry.

Various labile chemical bonds (chemical barriers) have been employed for the controlled release of a range of fragrant molecules, such as (a) the controlled release of alcohol using neighboring-group-assisted ester hydrolysis (De Saint Laumer, Frerot, & Herrmann, 2003), (b) the use of Schiff bases to help control the release of aldehydes and ketones (Kamogawa, Mukai, Nakajima, & Nanasawa, 1982; Turin, 2006; Muzzarelli & Ilari, 1994), (c) the use of Norrish type-II photofragmentation to control the delivery of alkenes and acetophenones (Levrand & Herrmann, 2002), carbonyl compounds (Levrand & Herrmann, 2007) and aldehydes and ketones (Rochat, Minardi, De Saint Laumer, & Herrmann, 2000), (d) the use of aminal (Godin, Levrand, Trachsel, Lehn, & Herrmann, 2010) or acetal (Morinaga, Morikawa, Wang, Sudo, & Endo, 2009) groups for the controlled release of aldehydes, (e) the use of hydrazone for the delivery of aldehydes and ketones (Levrand, Fieber, Lehn, & Herrmann, 2007; Levrand, Ruff, Lehn, & Herrmann, 2006), (f) the photo-assisted release of aldehydes from α-acetoxy ethers (Robles & Bochet, 2005) and (g) the slow release of enones through a Retro-Michael addition reaction (Fehr & Galindo, 2005).

Examples of physical barrier used in the prolongation of fragrances include double emulsion system (Edris & Bergnståhl, 2001), cyclodextrin host (Wang & Chen, 2005a, 2005b), mesoporous silica spheres (Wang, Zhu, Yang, & Chen, 2008), solid lipid nanoparticles (Souto & Müller, 2008), multi-arm star block copolymer (Ternat et al., 2007), various other synthetic polymers formed by miniemulsion polymerization (Landfester, 2009) and in situ polymerization (Lee, Lee, Cheong, & Kim, 2002), amphipilic crosslinked polymer network (Brown, Bergquist, Ferm, & Wooley, 2005) and various carbohydrates (Hambleton, Fabra, Debeaufort, Dury-Brun, & Voilley, 2009; Korus, Tomasik, & Lii, 2003; Paula, Sombra, Cavalcante, Abreu, & De Paula, 2011; Quellet, Schudel, & Ringgenberg, 2001). Fragrance prolongation technology for personal care and household product applications should not only

* Corresponding author. Tel.: +662 2187634; fax: +662 2541309.
E-mail address: psupason@chula.ac.th (S.P. Wanichwecharungruang).

0144-8617/$ – see front matter © 2011 Elsevier Ltd. All rights reserved.
doi:10.1016/j.carbpol.2011.06.074

provide long lasting fragrance but also possess no harm to the environment. The use of non-biodegradable non-biocompatible melamine-formaldehyde microspheres may pose environmental problem considering that they are now being used in many household products including laundry detergents and fabric softeners. However, reported systems based on biodegradable carbohydrates, such as alginate, starch and chitosan, in the form of water dispersible nanoparticles or microparticles neither provide enough physical stability nor show satisfactory fragrant prolongation.

Here, for the first time, we demonstrate the fabrication of long lasting fragrance controlled release systems which contain both chemical and physical barriers, based on the biocompatible biodegradable non-toxic chitosan polymer. The fabricated materials are double barrier nanospheres in which fragrant aldehyde molecules are chemically linked to the N-succinylchitosan (NS-chitosan) and at the same time embedded in the particles' core.

2. Materials and methods

2.1. Materials

Chitosan with a degree of deacetylation of 85% (M_v = 30,000 Da) was obtained from Seafresh Chitosan (Lab) Co., Ltd. (Bangkok, Thailand). Succinic anhydride, vanillin, citral and citronellal were purchased from Acros organics (Geel, Belgium). Cinnamaldehyde was purchased from Aldrich (Steinheim, Germany). All other chemicals were analytical grade reagents and were obtained locally.

2.2. Synthesis of N-succinylchitosan (NS-chitosan) (Scheme 1)

NS-chitosan was synthesized based on the previously described method (Zhu, Yuan, & Lu, 2007), with a slight modification. Chitosan (2.01 g) was dissolved in 70 ml of 2% (v/v) acetic acid. Then succinic anhydride (0.25 g) in 10 ml of acetone was dropped into the chitosan solution and the mixture was stirred at room temperature overnight before being precipitated, and repeatedly washed (after filtration) with an excess amount of acetone. The product was dried in desiccators at room temperature. The dry product was analyzed by attenuated total reflectance-Fourier transform infrared spectroscopy (ATR-FTIR; Nicolet 6700 FT-IR spectrometer, Thermo Electron Corporation, Madison, WI, USA), [^{1}H]-NMR in D_2O (400 MHz Varian mercury spectrometer, Variance Inc., Palo Alto, USA), X-ray diffraction spectrometry (XRD), using a Cu Kα radiation source and operating at 40 kV and 30 mA (Rigaku DMAX 2200/Ultima$^+$ diffractometer, Rigaku International Corporation, Tokyo, Japan) and UV–Vis spectroscopy in a one centimeter-path-length-quartz cell, thermostated at 25 °C (UV 2500 UV-Vis spectrophotometer, Shimadzu Corporation, Kyoto, Japan).

N-succinylchitosan (NS-chitosan). White powder. 75% yield. Degree of succinyl grafting: 0.18. [^{1}H]-NMR (D_2O, 400 MHz, δ, ppm): 2.01 (H of acetyl groups), 2.42–2.50 (methylene protons of the succinyl moiety), 2.80 (H2 of glucosamine, GlcN), 3.50–3.92 (H2′ of N-acetylglucosamine, GlcNAc, H3, H4, H5 and H6 of GlcNAc and GlcN) and 4.54 (H1 of GlcNAc and GlcN). ATR-FTIR (cm^{-1}): 3282 (N–H stretching and O–H stretching vibration), 2864 (C–H stretching vibration), 1652 (amide I (C=O stretching)), 1555 (amide II), 1406 (symmetric stretching vibration of COO^- and amide III), 1319 (amide III (C–N stretching)), 1143 (C–O–C stretching vibration) and 1027 (C–O stretching vibration). UV–Vis (distilled water, 25 °C) λ_{max}: 252 nm, ε: 0.0278 M^{-1} cm^{-1} per monomeric unit.

2.3. Characterization of the self-assembled NS-chitosan

A transparent colloidal suspension of NS-chitosan was easily obtained by simply dispersing the NS-chitosan in water: it was dried in desiccators at room temperature. The dry sample was subjected to the following analyses: *scanning electron microscopy* (SEM; JSM-6400 scanning electron microscope, JEOL, Tokyo, Japan), following gold coating under vacuum at 15 kV for 90 s and visualization at an accelerating voltage of 15 kV; *atomic force microscopy* (AFM; Nanoscope IV scanning probe microscope operated in tapping mode, Veeco Metrology Group, California, USA); *transmission electron microscopy* (TEM; JEM-2100, JEOL, Tokyo, Japan) operated at 100–120 kV; *X-ray photoelectron spectroscopy* (XPS; Kratos AXIS Ultra DLD instrument, Kratos, Manchester, England) using a monochromatic Al Kα X-ray source at 1486.6 eV and operated at 150 W, 15 kV and 10 mA with a base pressure in the XPS analysis chamber of 5×10^{-8} Torr. High resolution spectra (C1s and N1s) were acquired using a pass energy of 20 eV and 0.1 eV energy steps. All binding energies (BEs) were referenced to the hydrocarbon C1s peak at 285 eV. In addition, an aqueous suspension of NS-chitosan was used to evaluate the hydrodynamic diameter and zeta potential values (Zetasizer nanoseries model S4700, Malvern Instruments, Worcestershire, UK).

2.4. Synthesis of imine-NS-chitosan (Scheme 1)

NS-chitosan nanospheres were allowed to react with aldehyde at a 1:3 (w/w) ratio of aldehyde: NS-chitosan. The procedure involved adding 4 ml of alcoholic solution of 20% (v/v) aldehyde drop-wise to the aqueous NS-chitosan particle suspension (16 ml, 60 mg) under ultrasonic conditions. The mixture was further ultrasonicated (40 kHz at 30 °C) for 4 h. The product was dried in desiccators at room temperature and subjected to ATR-FTIR, SEM, AFM, TEM and XPS analyses.

N,N′-vanillidene-succinylchitosan nanospheres. Degree of vanillin substitution: 0.34. ATR-FTIR (cm^{-1}): 3282 (N–H stretching and O–H stretching vibration), 2867 (C–H stretching vibration), 1635 (C=N stretching vibration), 1592 and 1512 (C=C stretching vibration of aromatic), 1555 (amide II), 1143 (C–O–C stretching vibration) and 1027 (C–O stretching vibration).

N,N′-cinnamylidene-succinylchitosan nanospheres. Degree of cinnamaldehyde substitution: 0.29. ATR-FTIR (cm^{-1}): 3282 (N–H stretching and O–H stretching vibration), 2867 (C–H stretching vibration), 1632 (C=N stretching vibration), 1592 (C=C stretching vibration of aromatic), 1552 (amide II), 1147 (C–O–C stretching vibration) and 1024 (C–O stretching vibration).

N,N′-citronellalidene-succinylchitosan nanospheres. Degree of citronellal substitution: 0.38. ATR-FTIR (cm^{-1}): 3282 (N–H stretching and O–H stretching vibration), 2870 (C–H stretching vibration), 1638 (C=N stretching vibration), 1612 (C=C stretching vibration), 1552 (amide II), 1147 (C–O–C stretching vibration) and 1024 (C–O stretching vibration).

N,N′-citralidene-succinylchitosan nanospheres. Degree of citral substitution: 0.38. ATR-FTIR (cm^{-1}): 3282 (N–H stretching and O–H stretching vibration), 2874 (C–H stretching vibration), 1638 (C=N stretching vibration), 1612 (C=C stretching vibration), 1555 (amide II), 1143 (C–O–C stretching vibration) and 1027 (C–O stretching vibration).

2.5. Synthesis of imine-chitosan

N-vanilidenechitosan was synthesized *via* the Schiff reaction carried out with a 3:1 (w/w) ratio of chitosan to vanillin. Briefly, 20 mg of vanillin in 4 ml of ethanol was added drop-wise into a 16 ml of a 0.75% (w/v) aqueous chitosan solution in 2% (v/v) acetic acid. The mixture was continuously stirred without heat for 4 h and then the obtained product was dried in desiccators at room temperature and the dry product was subjected to ATR-FTIR and XPS analyses.

N-vanillidenechitosan. ATR-FTIR (cm^{-1}): 3289 (N–H stretching and O–H stretching vibration), 2877 (C–H stretching vibration),

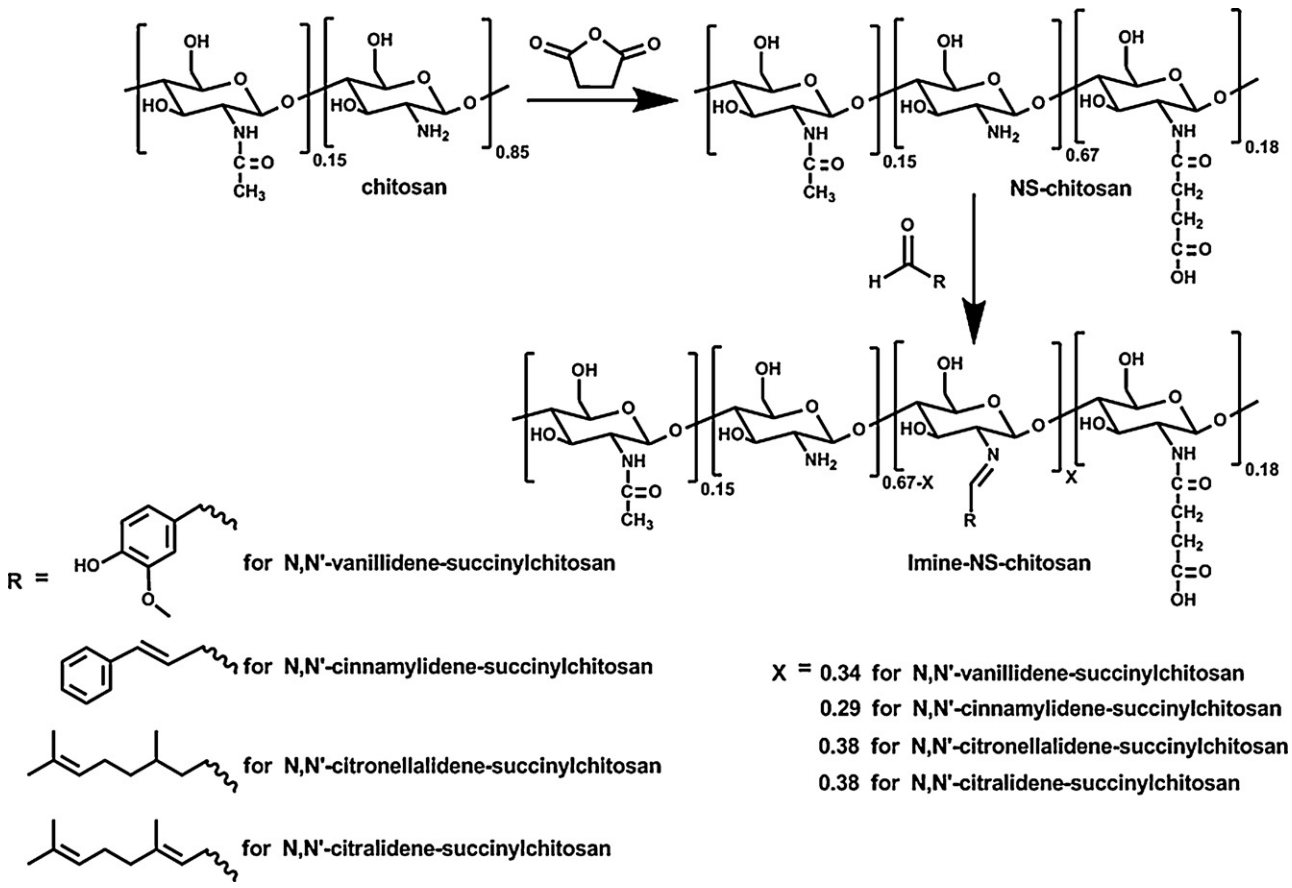

Scheme 1. Synthesis and structural details of NS-chitosan and imine-NS-chitosan from chitosan.

1635 (C=N stretching vibration), 1592 and 1512 (C=C stretching vibration of aromatic), 1150 (C–O–C stretching vibration) and 1027 (C–O stretching vibration).

2.6. Critical aggregation concentration (CAC) determination by steady-state fluorescence spectroscopy

One ml of pyrene solution (10 μM in methanol) was placed in a test tube and the methanol was removed by evaporation under a nitrogen atmosphere. To this, 10 ml of an aqueous solution of NS-chitosan of various concentrations (0.05, 0.10, 0.15, 0.20, 0.25, 0.30, 0.35, 0.40, 0.45, 0.50, 0.55 and 0.6 mg/ml) was added into the test tube to obtain a 1 μM final concentration of pyrene. The mixture was left at room temperature overnight for equilibration before being subjected to spectrofluorometric analysis (λ_{excite} = 334 nm, the emission recorded from 350 to 450 nm, Varian Cary Eclipse spectrofluorometer, Varian Optical Spectroscopy Instruments, Mulgrave, Victoria, Australia). The emission spectra for imine-NS-chitosan were acquired using the same procedure as described above. All experiments were carried out in triplicate.

2.7. Determination of the release profiles

For each of the Schiff base nanoparticle aqueous dispersions (pH of 5.5, prepared from 37.5 mg NS-chitosan and 12.5 mg aldehyde), 5 ml were loaded in a 20 ml flat bottom-headspace-vial (seven vials for each sample). The vials were left uncovered at 32 °C (room temperature in Bangkok). Due to water evaporation, 20% (v/v) ethanol–water was added to each vial everyday to maintain a near constant volume throughout the 16-day experiment. At the indicated times (0, 1, 2, 5, 8, 12 and 16 days), one of the seven initial vials per sample was pH adjusted to 1.0 with 1 M HCl, filled with 15 ml of hexane and then capped with headspace aluminum crimp caps with PTFE/silicone septa. The hexane layer was then subjected to aldehyde quantification using UV–Vis spectroscopy with the aid of a calibration graph constructed from freshly prepared standard aldehyde solutions. The release of each free aldehyde was similarly tested using a sample vial containing 12.5 mg of aldehyde in 20% (v/v) ethanol–water.

The release of perfumery aldehydes was also evaluated in dry samples at 40 °C. Here 10 ml of the freshly prepared imine-NS-chitosan nanoparticle suspensions (prepared at final concentration of aldehyde of 2500 ppm) were left in the uncapped 20 ml flat bottom-headspace-vial for 60 days. Under this condition the samples became dry after 20 days, as no water was added into the vials, and the dry samples were kept at the same condition until the 60-day period was reached. Control samples were solutions of corresponding aldehydes at 2500 ppm (in 20% (v/v) ethanol–water). Then after 60 days, each sample vial was filled with 15 ml of 50% (v/v) ethanol–water, the sample was kept 24 h, and the ethanol–water phase was subjected to aldehyde quantification as described above.

3. Results and discussion

3.1. Chemical structure of N-succinylchitosan (NS-chitosan) (Scheme 1)

Successful grafting of the succinyl group onto the chitosan chain was confirmed through (i) the [^{1}H]-NMR spectrum of the product with the appearance of the resonance peaks at 2.42–2.50 ppm from the methylene protons of the grafted succinyl moiety (Fig. 1),

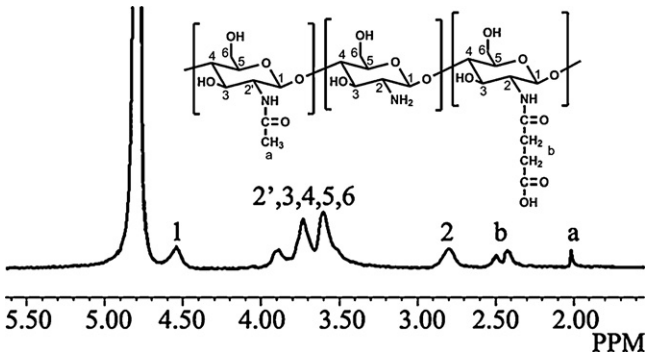

Fig. 1. [^{1}H]-NMR spectrum of NS-chitosan.

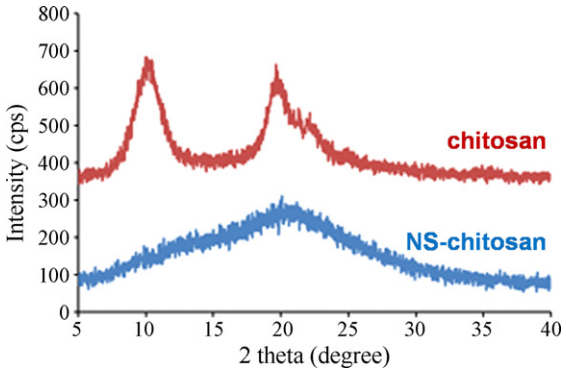

Fig. 3. X-ray powder diffraction patterns of chitosan and NS-chitosan.

and (ii) the FT-IR spectrum of the product with the appearance of the strong absorption peak at 1555 cm^{-1} which corresponded to amide II, an evident decrease of the peak at 1588 cm^{-1} ($-NH_2$ bending), and an appearance of the new absorption peak at 1406 cm^{-1} corresponding to the symmetric stretching vibration of COO^- and amide III (Fig. 2). The degree of grafting or succinyl substitution was estimated from the [^{1}H]-NMR spectrum using the ratio between the integrated area of the resonance peaks of the methylene protons of the grafted succinyl group, $I_{succinyl}$ ($-C(O)C\mathbf{H_2}C\mathbf{H_2}C(O)-$, 2.42–2.50 ppm) and that of the resonance peaks from hydrogen atoms at C2 in glucosamine units, I_{H2} (H2 of the Gln, 2.80 ppm). Taking into account the degree of deacetylation of 0.85 for the starting chitosan, the degree of succinyl grafting was approximated to be 0.18.

Chitosan is insoluble in water at a pH >6.5 because of its compact crystalline structure and strong intra- and inter-molecular H-bondings. The XRD pattern of chitosan possesses a distinct 2θ at 11° and 20° while that of the NS-chitosan shows a broad 2θ peak at 20° (Fig. 3). This information implied that NS-chitosan was significantly less crystalline than chitosan, which corresponds to the change in polymer packing structure and is ascribed to the disruption of H-bondings in the chitosan chains upon succinylation, and results in the freedom of NS-chitosan chains to self-assemble into particular suprastructures, as discussed below.

3.2. Morphology of NS-chitosan nanoparticles

A transparent colloidal suspension of NS-chitosan could easily be obtained by simply dispersing the NS-chitosan in water. The SEM and TEM images of the dried NS-chitosan preparation (Fig. 4) confirmed their spherical morphology when dry. The hydrodynamic diameter and zeta potential of the hydrated (aqueous suspension) NS-chitosan nanoparticles were 46.3 ± 0.24 nm (PDI of 0.1850) and 22.3 ± 2.6 mV, respectively (Fig. 4c).

The NS-chitosan aggregates are equilibrium structures that result from a balance of electrostatic repulsion, hydrophobic interactions and hydrogen bonding of functional groups in the NS-chitosan structures and water molecules. The hydrophilic functional groups of the NS-chitosan include the carboxylic acid, amide and free amino and hydroxy moieties on the GlcN units, while the hydrophobic functionalities include the diethylene ($-CH_2CH_2-$) units of the grafted succinyl moieties and the methylene groups of the sugar units.

3.3. Synthesis and characterization of imine-NS-chitosan

The objective of this work was to convert the obtained NS-chitosan nanospheres into double barrier carriers for the controlled release of perfumery aldehydes. Here, the chemical barrier could be successfully created *via* a Schiff base formation between the NS-chitosan nanospheres and the aldehydes by directly reacting the amino groups on the NS-chitosan spheres with the aldehydes. Four perfumery aldehydes consisting of two aromatic (vanillin and cinnamaldehyde) and two aliphatic (citral and citronellal) aldehydes were used and the products obtained were N,N′-vanillidene-succinylchitosan (van-NS-chitosan), N,N′-cinnamylidene-succinylchitosan (cin-NS-chitosan), N,N′-

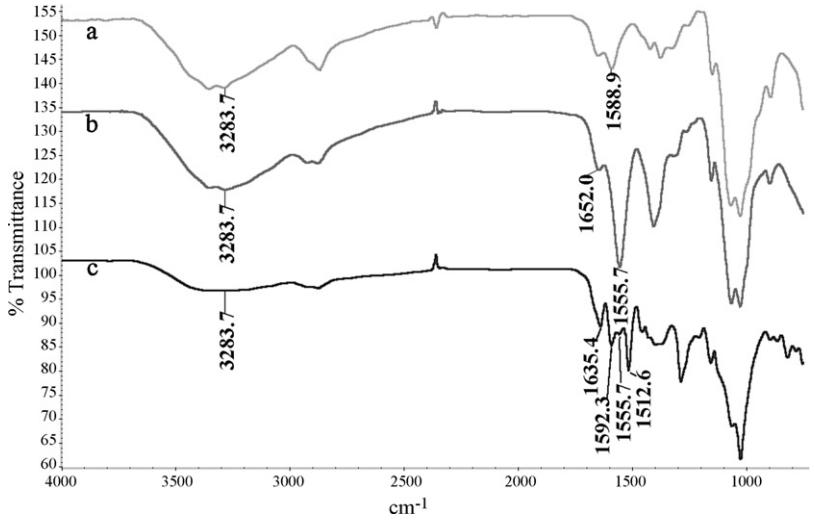

Fig. 2. ATR-FTIR spectra of (a) chitosan, (b) NS-chitosan and (c) van-NS-chitosan.

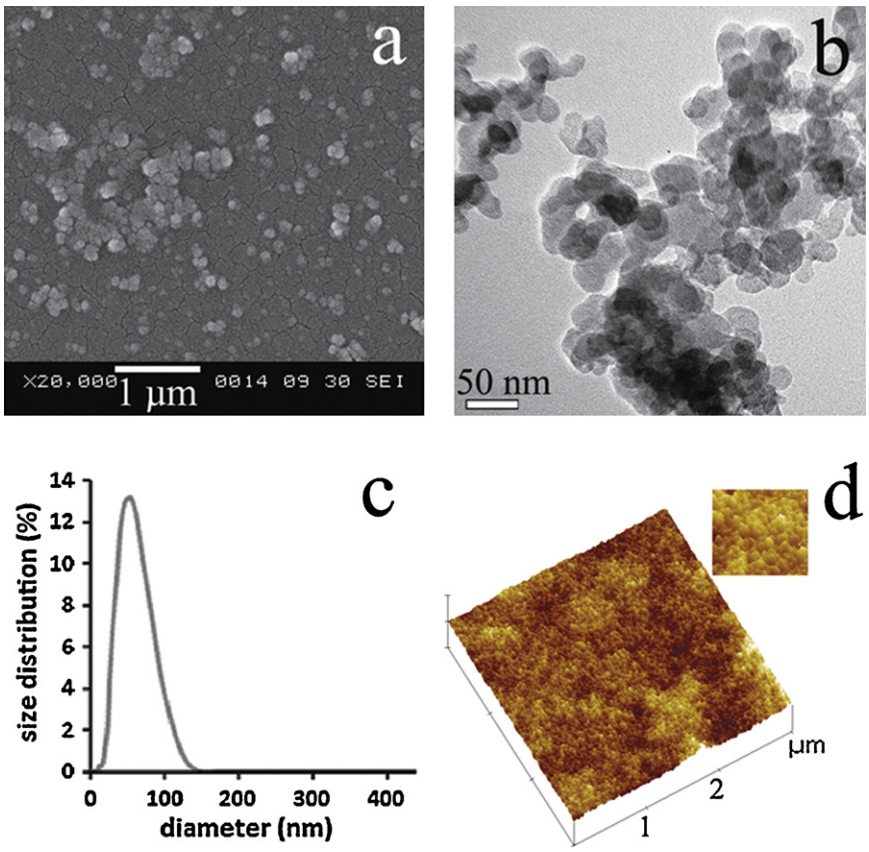

Fig. 4. (a) SEM image, (b) TEM image, (c) size distributions of NS-chitosan nanoparticles. (d) AFM image of van-NS-chitosan spheres.

citronellalidene-succinylchitosan (citro-NS-chitosan) and N,N′-citralidene-succinylchitosan (citral-NS-chitosan), respectively. Characterization of the product was carried out by FT-IR analysis: for the van-NS-chitosan product, new absorption peaks at 1635 cm^{-1}, and 1592 and 1512 cm^{-1}, corresponding to the C=N stretching of imine (Schiff base) and the C=C stretching vibration of the aromatic ring, respectively, together with the disappearance of the absorption peak at 1665 cm^{-1} that corresponds to the characteristic stretching vibration of the aryl aldehyde group, confirmed the successful synthesis and verified that no aldehyde functionality was left in the system (Fig. 2). Other Schiff base products based on cinnamaldehyde, citronellal and citral could also be successfully synthesized (see their FT-IR spectra in supplementary data). The experiment was carried out to obtain maximum mole ratio between aldehyde and NS-chitosan. Under the obtained condition, all aldehyde molecules were used up in the reaction (no aldehyde was detected in all four products, see details in supplementary data), thus it could be estimated that all four imine-NS-chitosan products possessed a degree of imine substitution in the range of approximately 0.29–0.38 (Scheme 1). To confirm this, each product was subjected to acid hydrolysis followed with quantitative analysis of the recovered aldehydes and the result agreed well with our estimation above. AFM images of the Schiff base products indicated a spherical morphology (Fig. 4d and more in supplementary data). AFM images of the Schiff base products clearly show undeformed spheres. The hydrodynamic diameter increased from 50 nm for NS-chitosan particles to 80–165 nm for the Schiff base NS-chitosan particles. The imine-NS-chitosan nanoparticles exhibited a higher zeta potential value than the NS-chitosan particles (Table 1). Comparing between aromatic aldehydes (vanillin and cinnamaldehyde) and aliphatic aldehydes (citral and citronellal), the former gave Schiff base spheres with larger diameters. This was not surprising because all four Schiff base products possessed a similar imine substitution degree but the two aromatic imine moieties are larger than the two aliphatic ones. The size of the spheres thus corresponded to the polymer chemical structures.

3.4. Critical micellar concentration

The critical aggregation concentration (CAC) of NS-chitosan and citro-NS-chitosan was determined using fluorescence spectroscopy by monitoring the assembly of the polymer in the presence of pyrene as the fluorescent probe and the results suggested the values in water of ≈0.2 mg/ml for NS-chitosan and citro-NS-chitosan, respectively (see supplementary data for more details). The CAC values were more than ten folds lower than the concentrations of the two materials in the reaction, thus confirming their aggregation state in the reaction.

3.5. Surface characterization by X-ray photoelectron spectroscopy (XPS)

We hypothesized that the grafted hydrophobic imine moieties should try to position themselves into the spherical cores,

Table 1
Characters of the imine-NS-chitosan particles.

Nanospheres	Hydrodynamic size		Zeta potential
	nm	PDI	mV
Van-NS-chitosan	163.4 ± 2.1	0.177	48.8 ± 1.7
Cin-NS-chitosan	130.9 ± 4.9	0.333	57.3 ± 4.6
Citro-NS-chitosan	109.6 ± 1.6	0.198	38.3 ± 2.4
Citral-NS-chitosan	80.9 ± 1.7	0.166	42.4 ± 0.65
NS-chitosan	46.3 ± 0.24	0.185	22.3 ± 2.6

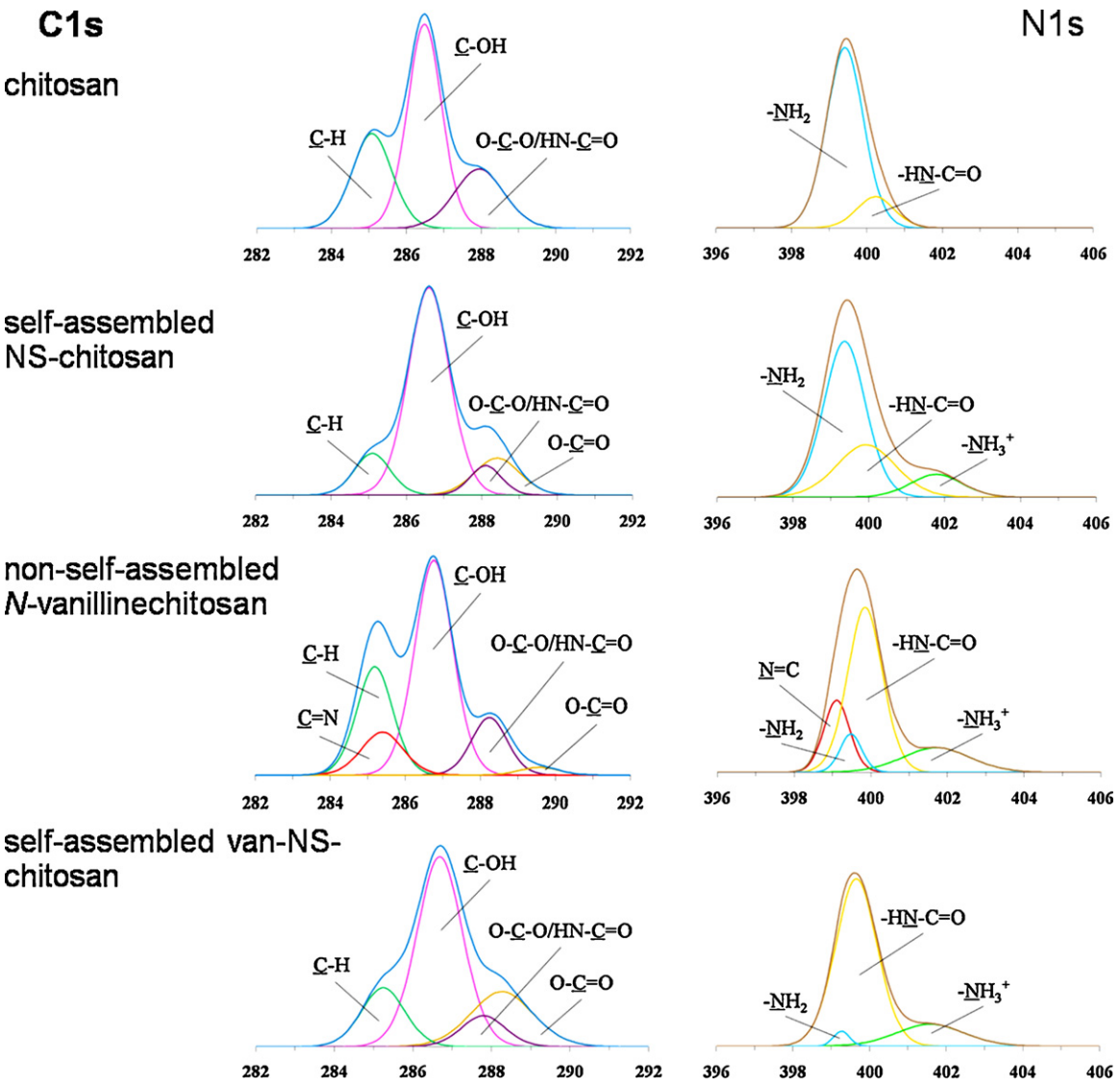

Fig. 5. XPS high resolution spectra of chitosan, self-assembled NS-chitosan, non-self-assembled N-vanillinechitosan and self-assembled van-NS-chitosan.

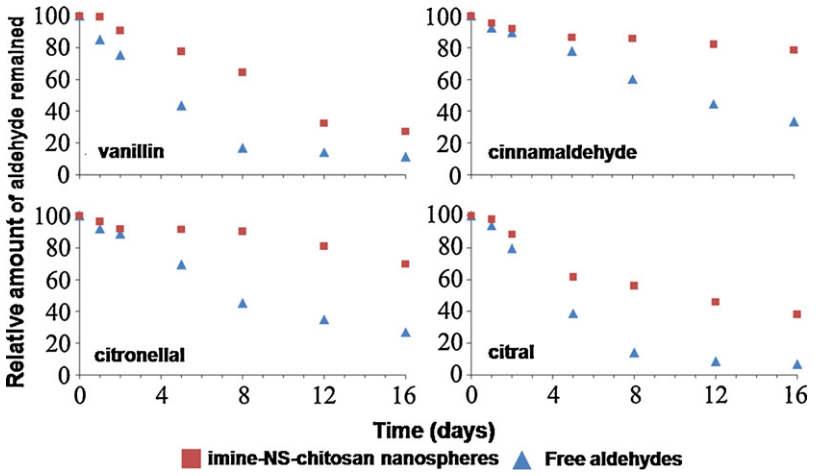

Fig. 6. The release of aldehydes from imine-NS-chitosan nanospheres in an aqueous suspension compared to the free aldehydes. The remaining unrelated imine moieties were quantified by UV-absorption analysis after acid hydrolysis. Data are shown as the mean + 1 SD.

away from being in direct contact with polar water medium. If this hypothesis is correct, a double barrier-carrier, in which the imine linkage was the chemical barrier and the polymeric matrix wall was the physical barrier, would have been successfully generated. Therefore, we investigated the location of the grafted imine groups in the obtained imine-NS-chitosan spheres. Here the XPS technique, which usually gives chemical composition data at the surface layer up to a thickness of approximately 8 nm, was employed.

Comparing to the NS-chitosan particles, X-ray photoelectron (XPS) analysis revealed more than 90% decrease in the amino functionality (relative to amide functionality) at the van-NS-chitosan particles' surface, but with no appearance of the C=N functionality (Fig. 5). Since the IR spectrum of the van-NS-chitosan particles showed prominent C=N functionality (1635 cm^{-1}), the C=N moieties were likely to be at the inside of the particles, more than 8 nm dept from the surface. This implied that, all the grafted perfumery moieties were at the core of the dry particles. Although the XPS analysis was performed on the dry particles (prepared through freeze-drying by quickly freezing the aqueous particle suspension at −80 °C and subjecting to high vacuum removal of water), the result should also represent the particles' structure in water too. This was because the reshuffling of the moieties in the particles during the freeze-drying, should be minimized. More importantly, since the air is much less polar than water, if the shuffling during the drying was to occur, it should be in the direction that the less polar moieties (the grafted imines) were shuffled up to the surface. But the result showed no imine on the particles' surface.

The localization of the grafted hydrophobic imine moieties at the particles' core occurred because of the drive towards the minimum free energy of the local equilibrium around the spheres. In other words, thermodynamically such organization took place in order to maximize hydrophobic interactions amongst the grafted hydrophobic moieties and to minimize contact between the polar medium (water) and the non-polar imine moieties. Kinetically the ultrasonication helped the system to be able to cross the chemical interactions within the NS-chitosan particles, and organized into the more thermodynamically stable architectures. It was possible that as the reaction was taking place firstly between the amino groups at the particles' surface and the incoming aldehyde molecules (XPS analysis of NS-chitosan particles showed abundant of amino functionality at the surface), simultaneously and continuously with the aid of ultrasonication, the particles reorganized to localize the grafted hydrophobic imine to the core, this then exposing more amino groups towards the surface of the particles and thus more imine could be formed, and finally all the formed imine moieties were shuffled into the core of the particles (no detection of imine functionality at the surface by XPS analysis but obvious imine peak in the FTIR spectrum).

With no succinyl moiety on the chitosan backbone, the obtained N-vanillidenechitosan could not self-assemble into spherical architecture (confirmed through AFM, TEM and SEM). With no self-organization, some of the imine functionality (C=N) should be observable by XPS as they should remain at the surface. The C1s and N1s spectra of this non-self-assembled N-vanillidenechitosan showed evident peaks of the imine bond (C=N) at 285.4 eV and 399.1 eV, in the N1s and C1s high resolution XPS spectra, respectively, indicating that the grafted imine moieties were not all covered by polymeric matrix, but rather significant amounts of them were at the surface of the material (see ESI). This result assured that the XPS technique could clearly detect the C=N functionality in a chitosan derivative and that the undetection of C=N functionality for the imine-NS-chitosan particles was because they were not at the particles' surface.

Therefore, it is most likely that the proposed double barrier–carrier was successfully fabricated through a one step process in which the formation of imine linkages between the amino groups and aldehydes of the NS-chitosan nanospheres occurred in concerted with the localization of the grafted imine moieties at the particles' core.

3.6. Release of aldehydes

Since the imine-NS-chitosan nanospheres were designed to be double barrier fragrance controlled release systems in which the imine bond was a chemical barrier while the polymer shell was a physical barrier, the aldehyde release behavior of the four water suspension products was monitored by quantification amounts of the grafted imine that remained in the sample after incubation at 32 °C for up to 16 days. The remaining imine moieties were quantified by subjecting each sample to an acid-based imine hydrolysis to generate aldehydes and the generated aldehydes were then extracted with hexane and quantified by UV absorption spectroscopy. The prolonged release of aldehyde molecules could be observed both in the freeze-dry sample and in the aqueous suspension of the samples. The aqueous suspension system showed evident slow down release (Fig. 6). The release of the fragrant aldehydes from the dry samples was evaluated after being kept at 40 °C for 60 days. Hydrolysis of the samples followed with aldehyde quantification indicated (mean ± SD) 2.88 ± 0.20, 0.77 ± 0.02, 4.52 ± 0.31 and 1.31 ± 0.10 mg of vanillin, cinnamaldehyde, citronellal and citral in the corresponding imine-NS-chitosan samples, which was significantly higher (79.9-, 85.4-, 20.1- and 29.1-fold, respectively) than the free aldehyde levels in the control samples at 0.036 ± 0.001, 0.009 ± 0.002, 0.225 ± 0.092 and 0.045 ± 0.002 mg of vanillin, cinnamaldehyde, citronellal and citral, respectively. Note that each imine-NS-chitosan particles were prepared using 25 mg aldehyde and 25 mg of each corresponding aldehyde was used for the free aldehyde control sample. Comparing the release characteristic of the dry to that of the aqueous suspension samples, it was evident that the prolonged release of the double barrier systems was much more pronounced in the dry state. This was because the imine hydrolysis needs water molecules and there was much less availability of the water molecules for the dry samples.

4. Conclusion

Here a novel double barrier–carrier for fragrance aldehyde molecules was successfully created from biocompatible biodegradable chitosan polymer. The system contained a chemical barrier, in which the fragrance aldehydes were linked to the NS-chitosan *via* imine linkages, and a physical barrier, in which the grafted imine moieties were buried inside the chitosan matrix. Prolonged release of perfumery aldehydes was demonstrated both in a water suspension and, especially, in the dry state.

Acknowledgements

The authors thank the Development and Promotion of Science and Technology talents project (DPST), the Commission of Higher Education-Thailand Research Fund (BRG5280004), the Special Task Force for Activating Research (STAR) from the centenary academic development project, Chulalongkorn University, and the Thai Government Stimulus Package 2 (TKK2555) under the Project for Establishment of Comprehesive Center for Innovative Food, Health Products and Agriculture, for financial support. The authors also thank Professor Masayuki Yamaguchi and Mr. Murakami Tatsuya (School of Material Science, Japan Advanced Institute of Science and Technology, Japan) for the XPS analysis.

Appendix A. Supplementary data

Supplementary data associated with this article can be found, in the online version, at doi:10.1016/j.carbpol.2011.06.074.

References

Brown, G. O., Bergquist, C., Ferm, P., & Wooley, K. L. (2005). Unusual, promoted release of guests from amphiphilic cross-linked polymer networks. *Journal of the American Chemical Society*, *127*, 11238–11239.

De Saint Laumer, J. Y., Frerot, E., & Herrmann, A. (2003). Controlled release of perfumery alcohols by neighboring-group participation. Comparison of the rate constants for the alkaline hydrolysis of 2-acyl-, 2-(hydroxymethyl)-, and 2-carbamoylbenzoates. *Helvetica Chimica Acta*, *86*, 2871–2899.

Edris, A., & Bergnståhl, B. (2001). Encapsulation of orange oil in a spray dried double emulsion. *Die Nahrung*, *45*, 133–137.

Fehr, C., & Galindo, J. (2005). Aldols by Michael addition: Application of the retro-Michael addition to the slow release of enones. *Helvetica Chimica Acta*, *88*, 3128–3136.

Godin, G., Levrand, B., Trachsel, A., Lehn, J. M., & Herrmann, A. (2010). Reversible formation of aminals: A new strategy to control the release of bioactive volatiles from dynamic mixtures. *Chemical Communications*, *46*, 3125–3127.

Hambleton, A., Fabra, M. J., Debeaufort, F., Dury-Brun, C., & Voilley, A. (2009). Interface and aroma barrier properties of iota-carrageenan emulsion-based films used for encapsulation of active food compounds. *Journal of Food Engineering*, *93*, 80–88.

Herrmann, A. (2007). Controlled release of volatiles under mild reaction conditions: From nature to everyday products. *Angewandte Chemie – International Edition*, *46*, 5836–5863.

Kamogawa, H., Mukai, H., Nakajima, Y., & Nanasawa, M. (1982). Chemical release control – Schiff bases of perfume aldehydes and aminostyrenes. *Journal of Polymer Science – Polymer Chemistry Edition*, *20*, 3121–3129.

Korus, J., Tomasik, P., & Lii, C. Y. (2003). Microcapsules from starch granules. *Journal of Microencapsulation*, *20*, 47–56.

Landfester, K. (2009). Miniemulsion polymerization and the structure of polymer and hybrid nanoparticles. *Angewandte Chemie – International Edition*, *48*, 4488–4508.

Lee, H. Y., Lee, S. J., Cheong, I. W., & Kim, J. H. (2002). Microencapsulation of fragrant oil via in situ polymerization: Effects of pH and melamine-formaldehyde molar ratio. *Journal of Microencapsulation*, *19*, 559–569.

Levrand, B., & Herrmann, A. (2002). Light induced controlled release of fragrances by Norrish type II photofragmentation of alkyl phrnyl ketones. *Photochemical and Photobiological Sciences*, *1*, 907–919.

Levrand, B., Ruff, Y., Lehn, J. M., & Herrmann, A. (2006). Controlled release of volatile aldehydes and ketones by reversible hydrazone formation – "classical" profragrances are getting dynamic. *Chemical Communications*, 2965–2967.

Levrand, B., Fieber, W., Lehn, J. M., & Herrmann, A. (2007). Controlled release of volatile aldehydes and ketones from dynamic mixtures generated by reversible hydrazone formation. *Helvetica Chimica Acta*, *90*, 2281–2314.

Levrand, B., & Herrmann, A. (2007). Controlled light-induced release of volatile aldehydes and ketones by photofragmentation of 2-oxo-(2-phenyl)acetates. *Chimia*, *61*, 661–664.

Morinaga, H., Morikawa, H., Wang, Y., Sudo, A., & Endo, T. (2009). Amphiphilic copolymer having acid-labile acetal in the side chain as a hydrophobe: controlled release of aldehyde by thermoresponsive aggregation – dissociation of polymer micelles. *Macromolecules*, *42*, 2229–2235.

Muzzarelli, R. A. A., & Ilari, P. (1994). Chitosans carrying the methoxyphenyl functions typical of lignin. *Carbohydrate Polymers*, *23*, 155–160.

Paula, H. C. B., Sombra, F. M., Cavalcante, R. D. F., Abreu, F. O. M. S., & De Paula, R. C. M. (2011). Preparation and characterization of chitosan/cashew gum beads loaded with Lippia sidoides essential oil. *Materials Science and Engineering C*, *31*, 173–178.

Quellet, C., Schudel, M., & Ringgenberg, R. (2001). Flavors & fragrance delivery systems. *Chimia*, *55*, 421–428.

Robles, J. L., & Bochet, C. G. (2005). Photochemical release of aldehydes from α-acetoxy nitroveratryl ethers. *Organic Letters*, *7*, 3545–3547.

Rochat, S., Minardi, C., De Saint Laumer, J. Y., & Herrmann, A. (2000). Controlled release of perfumery aldehydes and ketones by Norrish type-II photofragmentation of α-keto esters in undegassed solution. *Helvetica Chimica Acta*, *83*, 1645–1671.

Souto, E. B., & Müller, R. H. (2008). Cosmetic features and applications of lipid nanoparticles (SLN®, NLC®). *International Journal of Cosmetic Science*, *30*, 157–165.

Ternat, C., Kreutzer, G., Plummer, C. J. G., Nguyen, T. Q., Herrmann, A., Ouali, L., et al. (2007). Amphiphilic multi-arm star-block copolymers for encapsulation of fragrance molecules. *Macromolecular Chemistry and Physics*, *208*, 131–145.

Turin, L. (2006). *WO Patent 2006/012215*. Flexitral Inc. [Chem. Abstr. 2006, 144, 176961].

Wang, C. X., & Chen, S. L. (2005a). Aromachology and its application in the textile field. *Fibres and Textiles in Eastern Europe*, *13*, 41–44.

Wang, C. X., & Chen, S. L. (2005b). Fragrance-release property of ß-cyclodextrin inclusion compounds and their application in aromatherapy. *Journal of Industrial Textiles*, *34*, 157–166.

Wang, P., Zhu, Y., Yang, X., & Chen, A. (2008). Prolonged-release performance of perfume encapsulated by tailoring mesoporous silica spheres. *Flavour and Fragrance Journal*, *23*, 29–34.

Zhu, A., Yuan, L., & Lu, Y. (2007). Synthesis and aggregation behavior of N-succinyl-o-carboxymethylchitosan in aqueous solutions. *Colloid and Polymer Science*, *285*, 1535–1541.